PAPER

ITER-like vertical stabilization system for the east Tokamak

To cite this article: R. Albanese *et al* 2017 *Nucl. Fusion* **57** 086039

IOP Publishing | International Atomic Energy Agency Nuclear Fusion
Nucl. Fusion 57 (2017) 086039 (10pp) https://doi.org/10.1088/1741-4326/aa7a78

ITER-like vertical stabilization system for the east Tokamak

R. Albanese[1,3], R. Ambrosino[2,3], A. Castaldo[1,3], G. De Tommasi[1,3], Z.P. Luo[4], A. Mele[1,3], A. Pironti[1,3], B.J. Xiao[4] and Q.P. Yuan[4]

[1] Dipartimento di Ingegneria Elettrica e delle Tecnologie dell'Informazione, Università degli Studi di Napoli Federico II, via Claudio 21, 80125, Napoli, Italy
[2] Dipartimento di Ingegneria, Università degli Studi di Napoli Parthenope, Centro Direzionale di Napoli, Isola C4, 80143 Napoli, Italy
[3] Consorzio CREATE, via Claudio 21, 80125, Napoli, Italy
[4] Institute of Plasma Physics, Chinese Academy of Sciences, Hefei 230031, People's Republic of China

E-mail: detommas@unina.it

Received 17 February 2017, revised 3 May 2017
Accepted for publication 20 June 2017
Published 14 July 2017

Abstract

A *ITER-like* vertical stabilization (VS) algorithm has been successfully deployed and commissioned at EAST. The proposed algorithm decouples the VS from the plasma shape control, while the algorithms previously implemented to stabilize the EAST plasma exhibit a strong coupling with plasma shape control system. As a consequence, the VS algorithms previously implemented at EAST prevent the deployment of advanced multi-input-multi-output (MIMO) plasma shape control schemes, such as the ones proposed in Albanese *et al* 2016 (*Proc. 2016 IEEE Multi-Conf. System Control (Buenos Aires, Argentina)* pp 611–6) and Kolemen *et al* (2015 *J. Nucl. Mater.* **463** 1186). Indeed, such MIMO controllers rely on the decoupling with the VS system.

The proposed *ITER-like* stabilizes the plasma column (i.e. it controls to zero the plasma vertical speed) on the fastest possible time scale, while leaves the control of the plasma vertical position to the plasma shape controller. Thanks to this *frequency separation* approach, the plasma shape controller can than be designed starting from the stabilized system, without explicitly taking the VS into account. In this paper we present the implementation details of the adopted solution for the EAST vertical stabilization, together with the results obtained during the 2016 experimental campaign.

Keywords: vertical stabilization system, plasma magnetic control, control systems, EAST tokamak

(Some figures may appear in colour only in the online journal)

1. Introduction

When solving the plasma magnetic control problem [3], the decoupling between the vertical stabilization (VS) system and the plasma shape and position control is essential to deploy advanced advanced plasma shape control schemes, such as [1, 2].

In particular, the multi-input-multi-output (MIMO) architecture for the integrated control of the plasma shape and of the heat flux presented in [1], aims at controlling advanced configurations at EAST, such as the quasi snowflake [4, 5], and is based on the extreme shape controller (XSC) design procedure [6–8]. Such an architecture strongly relies on the decoupling between the VS system and the plasma shape control, which is typically achieved by means of a frequency separation approach, implying that the design of the plasma current and position controller can be performed assuming a vertically stabilized plasma [9]. Moreover, having a decoupled architecture simplifies the design of the plasma shape and position control algorithm, otherwise the VS system should be taken explicitly into account during the design.

As a matter of fact, the existing EAST VS system [10, 11] does not always guarantee the decoupling between VS and plasma shape and position control. The undesired coupling prevents the deployment of advanced plasma shape control schemes such as [1, 2]. For this reason, the ITER-like VS algorithm proposed in [12, 13] has been deployed and tested at EAST in 2016. Such VS system, allows to achieve the desired decoupling, hence enabling the development of the *XSC-like* MIMO controller proposed in [1].

In this work the ITER-like solution for vertical stabilization is presented, together with the results obtained at EAST during the 2016 experimental campaign. In particular, the paper is structured as follows: the next section introduces the EAST magnetic control system and motivates the need of the proposed solution for vertical stabilization, whose details are given in section 3. The experimental validation of the proposed approach is presented in section 4, while some conclusive remarks are given in section 5.

2. Preliminaries

In this section, we first give a brief a introduction of the magnetic control system implemented within the EAST PCS (for the interested reader, a detailed description can be found in [10] and [11]). In the second part, we motivate the need of the proposed ITER-like VS system.

2.1. EAST magnetic control system

Plasma magnetic control at EAST is achieved by driving the required currents in the poloidal field (PF) coil system. Figure 1 shows the poloidal cross-section of the EAST tokamak with the layout of the PF coils. The 14 superconductive coils (PF1-14) are connected to form 12 independent PF circuits (the couples PF7/PF9 and PF8/PF10 are connected in series). The EAST PF coils system includes also two in-vessel copper coils (*IC*1 and *IC*2), that are connected in anti-series to form the so called *IC* circuit. This circuit is able to react to the plasma vertical instability on a faster time scale, if compared with the ex-vessel superconductive coils.

It is worth to notice that the EAST PF coils system has many technical similarities with the ITER one, i.e. it has a very similar layout; this makes the experience achieved on this machine relevant in view of ITER operation.

The EAST magnetic control system is implemented within the same software infrastructure adopted for the DIII-D PCS [14], and is constantly under development in order to satisfy growing experimental needs. Within the EAST PCS, the magnetic control system includes the following subsystems:

- the poloidal field circuit (PFC) Current Controller, that drives the currents in the superconductive ex-vessel coils;
- the plasma current controller, that tracks the plasma current reference waveform, by generating the correspondent requests to the PFC current controller;
- the shape and position controller, that tracks the shape of the plasma boundary or the position of the centroid, by generating the corresponding requests for the PFC current controller;

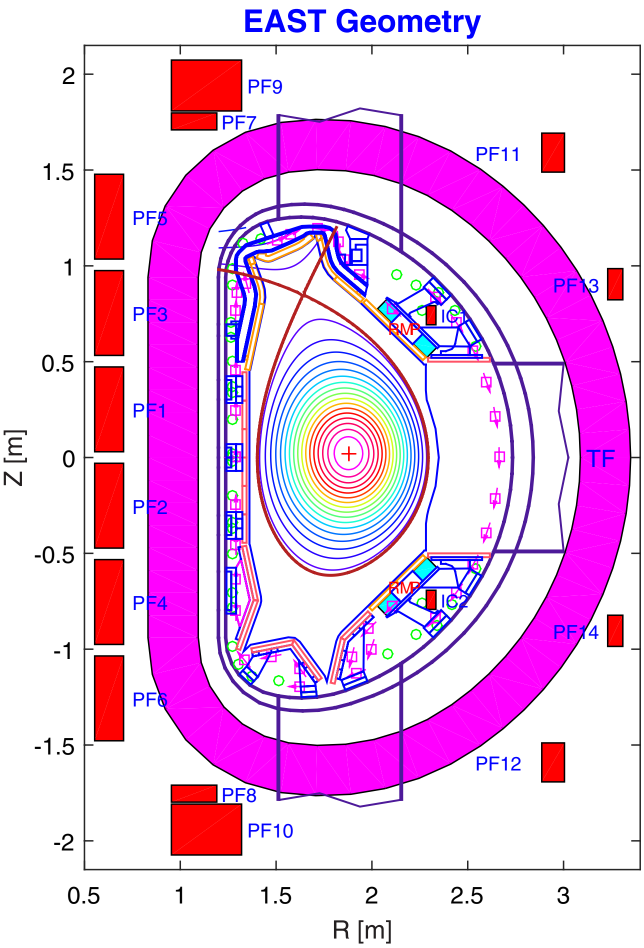

Figure 1. EAST poloidal cross-section and layout of the PF coils system. Both the ex-vessel PF superconductive coils and the in-vessel copper coils are shown. In this figure a upper single-null equilibrium is reported.

- the VS system, that drives the current in the in-vessel coil in order to vertically stabilize the plasma column.

A simplified block diagram of the EAST PCS architecture is shown in figures 2 and 3. In particular, the simplified block diagram of the plasma current and shape control system is reported in figure 2, where the targets for the PFC current controller are obtained as a sum of: (i) the requests computed by the plasma current controller $I_{\mathrm{PF}_{\mathrm{ref}_1}}$, (ii) the requests computed by plasma shape and position controller $I_{\mathrm{PF}_{\mathrm{ref}_2}}$, and (iii) the scenario feedforward I_{FF}.

The plasma current controller regulates the plasma current I_p by computing the set of current references $I_{\mathrm{PF}_{\mathrm{ref}_1}}$, which is then sent to the PFC current controller. Similarly, the plasma shape and position controller computes another set of additional references $I_{\mathrm{PF}_{\mathrm{ref}_2}}$. Two algorithms are currently available for plasma shape and position control, namely:

(spc1) *RZIP* control, that aims at controlling the position (both radial and vertical) of the plasma centroid; usually only four PF circuits (the ones that feed the coils PF11-PF14) are used as actuators to control the centroid position. The other PF circuits are used only for plasma current control.

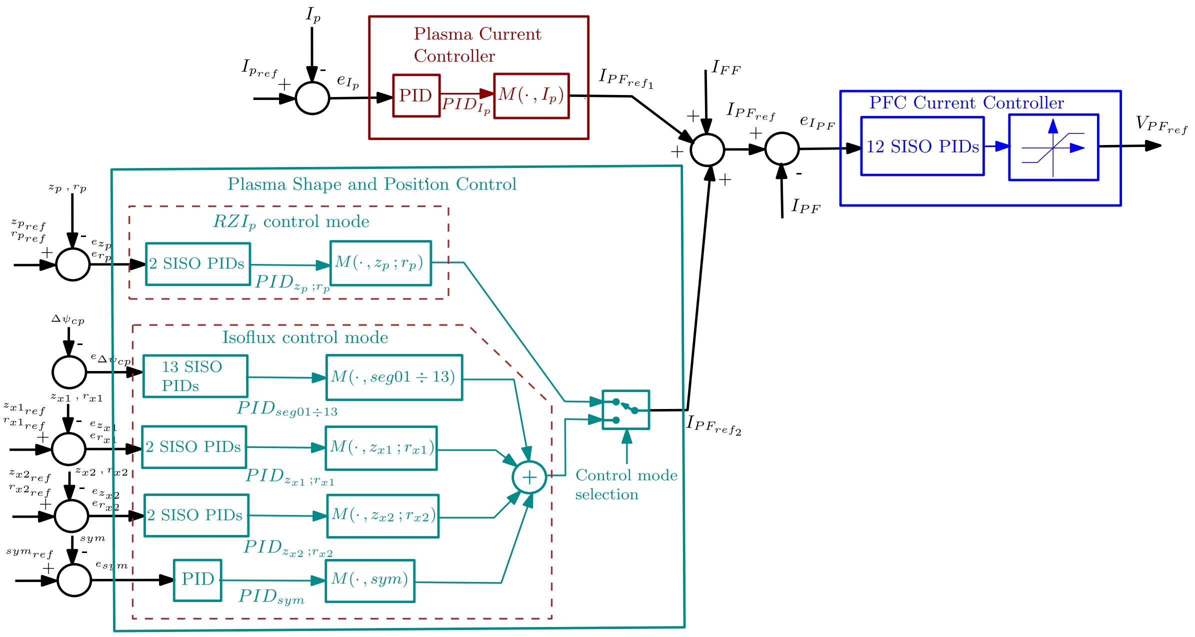

Figure 2. Simplified block diagram of the EAST plasma current, shape and position controllers. The M matrix is used to spread the contribution of each control loop among the 12 available PF circuits. The PF current requests are then tracked by the PFC current controller.

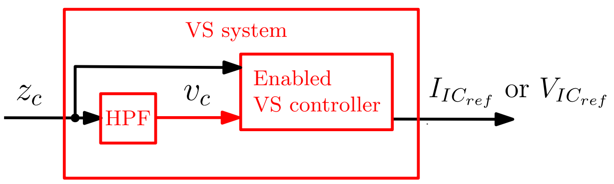

Figure 3. Simplified block diagram of the EAST vertical stabilization (VS) system. The EAST VS system takes as input the estimation of the plasma vertical displacement, and computes its derivative by filtering this estimation. Plasma vertical position and speed are then processed by the vertical stabilization controller, that can generate either a current or a voltage request for the *IC* power supply, according to the enabled algorithm.

(spc2) isoflux control, that aims at controlling the shape of the plasma boundary, by controlling the position of the *X*-point (upper and/or lower, depending on the chosen configuration), and by regulating to zero the flux error on a set of control segments. In order to control double-null plasmas, the isoflux control mode includes the *symmetry* loop, that is used to regulate the flux difference between the upper and lower *X*-point. The isoflux algorithms makes use of all the PF circuits, sharing them with the plasma current control.

All the control loops described so far, make use of proportional-integral-derivative (PID) controllers, which are usually experimentally tuned in order to obtain the desired closed-loop behaviour. For each control channel of both the plasma current and plasma shape and position controller, the PID outputs are distributed over the 12 available superconductive circuits, by using the weights specified into the correspondent column of the so-called M matrix. According to the usual design approach adopted at EAST, the M matrix results in a sparse matrix, since each controlled variables is linked to a subset of PF circuits.

The VS system, whose simplified block diagram is shown in figure 3, drives the current into the in-vessel copper coils. It sends either a voltage or a current request to the power supply of the *IC* circuit, depending on the control algorithm selected by the operator.

Before the implementation of the ITER-like control algorithm, which will be described in section 3, the VS system took as input the estimation of the plasma vertical displacement z_c and its derivative v_c, which is computed by using a derivative filter. In particular, the Laplace transform of the estimated plasma vertical speed is given by

$$V_c(s) = \frac{s}{1 + s\tau_z} Z_c(s),$$

where the time constant τ_z is usually set equal to 1 ms. Furthermore, the operator could choose among the following three different control algorithms:

(vs1) *PID control with IC in current-driven mode*; in this case the estimation of the plasma vertical speed is used as input to a PID with a pre-filter that computes the reference $I_{IC_{\rm ref}}$ as

$$I_{IC_{\rm ref}}(s) = \frac{1}{1 + s\tau_p} \cdot \left(K_p + \frac{K_i}{1 + s\tau_i} + \frac{K_d s\tau_d}{1 + s\tau_d} \right) \cdot V_c(s), \tag{1}$$

where K_p, K_i, and K_d are the PID gains, τ_p is the time constant for the low-pass pre-filtering, while τ_i and τ_d are the time constants for the integral and derivative actions, respectively. The target for the *IC* current computed as in (1) is then tracked by the local controller of the *IC* power supply. It is worth to notice that the *extended* PID (1) is the one provided within the PCS software library [14], and that the integral action is obtained as a low-pass filter with a time constant τ_I. Such a time constant is usually set to a value that is greater than the duration of the EAST

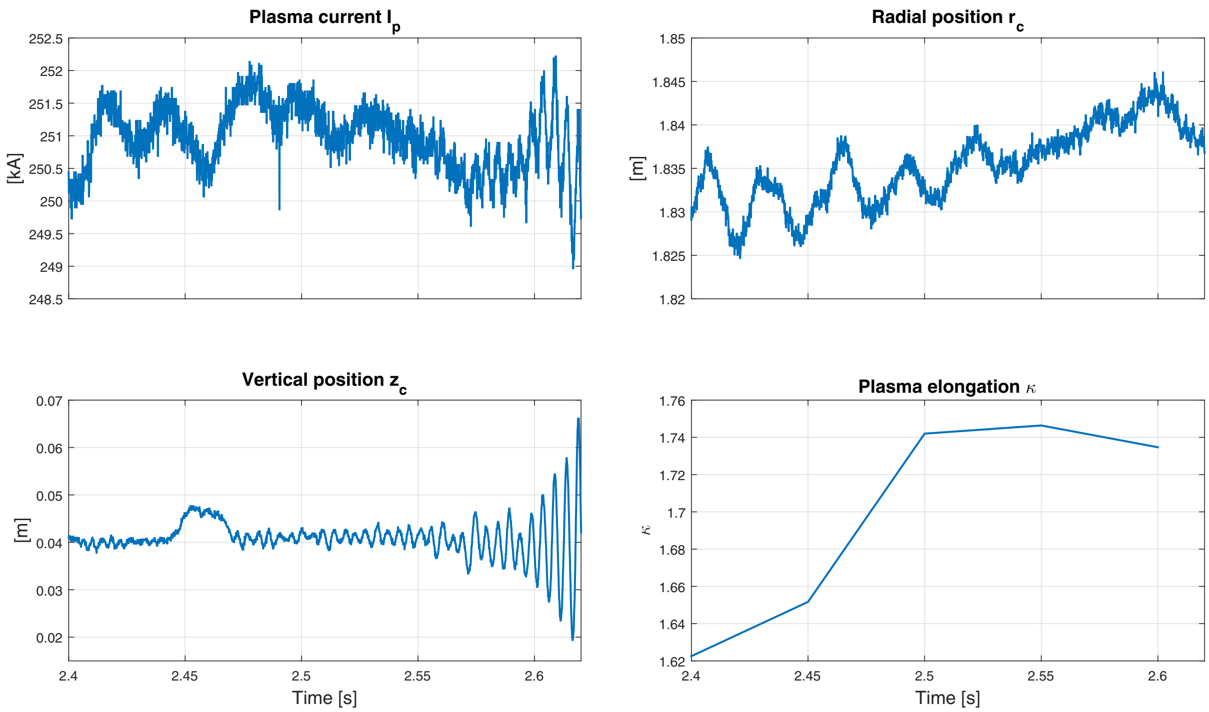

Figure 4. Time evolution plasma current I_{p}, plasma centroid position (both radial r_c and vertical z_c), and plasma elongation κ during the EAST pulse #69516. During this pulse the *IC* circuit was driven by the voltage-driven PID **(vs2)** while *RZIP* was used for plasma shape and position control. It can be noticed that these two system were not capable to vertically stabilize the plasma.

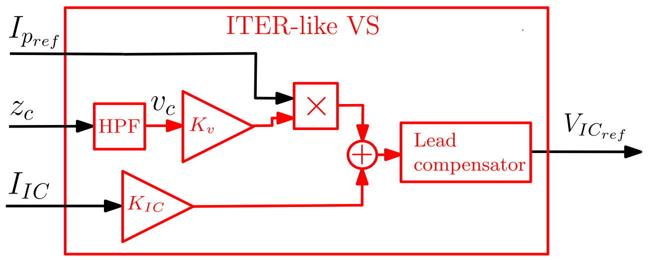

Figure 5. Simplified block diagram of the ITER-like vertical stabilization (VS) deployed at EAST. Differently from the EAST VS described in section 2.1, this scheme does not control the vertical position z_c, since only its derivative v_c is fed back. Moreover, it controls also the current flowing in the *IC* circuit, in order to minimize the Joule losses in the copper in-vessel coils. The target waveform for the plasma current $I_{p_{\mathrm{ref}}}$ is needed to scale the speed gain K_v.

pulse. Moreover, when used for vertical stabilization, the value of τ_p is set to a value corresponding to a cut-off frequency that is greater than the bandwidth of the VS system itself.

(vs2) *PID control with IC in voltage-driven mode*; this algorithm is similar to the previous one, but the PID output is the voltage reference $V_{IC_{\mathrm{ref}}}$ for the *IC* power supply.

(vs3) *Bang-bang control with IC in voltage-driven mode*; when this controller is enabled, the estimations of both the vertical position and speed are used as inputs to a bang–bang controller. In particular, when the control error on the position exceeds a threshold, then the bang–bang logic is used to drive the *IC* voltage. Otherwise, when the control error is within a given range, a voltage-driven PID controller is adopted (more details can be found in [11]).

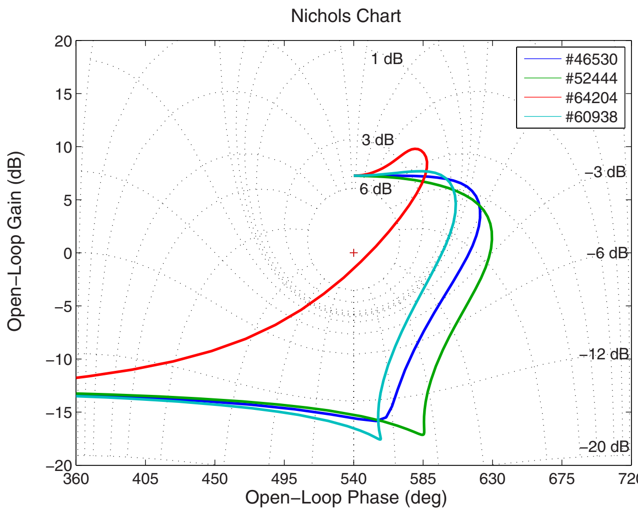

Figure 6. Nichols diagrams of the open loop transfer function at the output of the VS system shown in figure 5, for the four plasma equilibria listed in table 1, when the control parameters of ITER-like VS system are set equal to (3).

It is worth to remark that, all the VS algorithms listed above do not only stabilize the plasma, but also try to control the plasma vertical position, either directly as the bang–bang controller, or indirectly by means of the PID integral action on v_c. This fact implies a coupling between the VS system and the plasma current, Shape and Position control system,

Table 1. Main plasma parameters for the four equilibria considered to check stability when the ITER-like VS control parameters are set as in (3). The values reported for the growth rate γ, the elongation κ, the poloidal beta β_p, and the internal inductance l_i are the ones computed with the CREATE-NL equilibrium code [17].

Equilibrium	Shape type	$I_{P_{eq}}$ (kA)	γ [s^{-1}]	κ	β_p	l_i
46530 at $t = 3$ s	Double-null	281	137	1.66	0.30	1.27
52444 at $t = 3$ s	Limiter	230	92	1.35	0.26	1.34
60938 at $t = 6$ s	Upper single-null	374	194	1.77	0.78	0.95
64204 at $t = 3.5$ s	Lower single-null	233	512	1.61	0.02	2.19

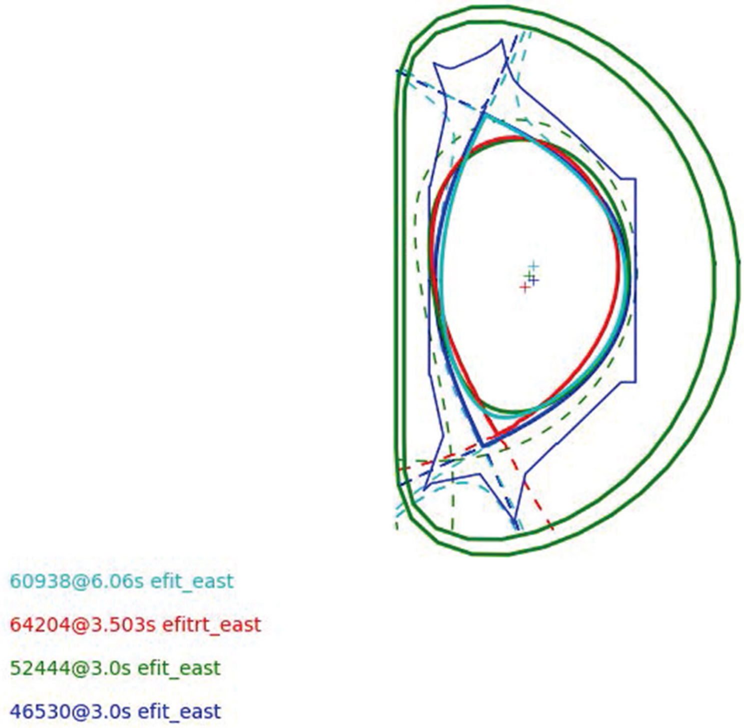

Figure 7. Plasma cross section for the four equilibria reported in table 1. It should be noticed that equilibrium #64204 occupies less volume and has also the greatest plasma-wall clearance with respect to the other considered equilibria; indeed this equilibrium is also the one with the highest growth rate, as reported in table 1.

which prevents to independently design the two systems, as it is better discussed in the next section.

2.2. Motivations

In [1] a MIMO plasma shape control algorithm has been proposed for the EAST tokamak. Such a solution exploits the same software architecture of the plasma shape and position controller described in section 2.1. In particular, the MIMO controller described in [1] can be implemented by configuring the control parameters of the EAST isolfux algorithm.

The main difference between the existing isoflux shape controller and the one proposed in [1], is that in the latter the *M* matrix is designed according to the singular value decomposition of the linearized relationship between the controlled variables and the currents in the PF circuits. Such a model-based design procedure minimizes the square mean error on the controlled variables [12, 15]. Furthermore, thanks to this approach, it is possible to control a number of plasma parameters greater than the number of available PF circuits (as it is done in the case of the XSC at the JET Tokamak [16]).

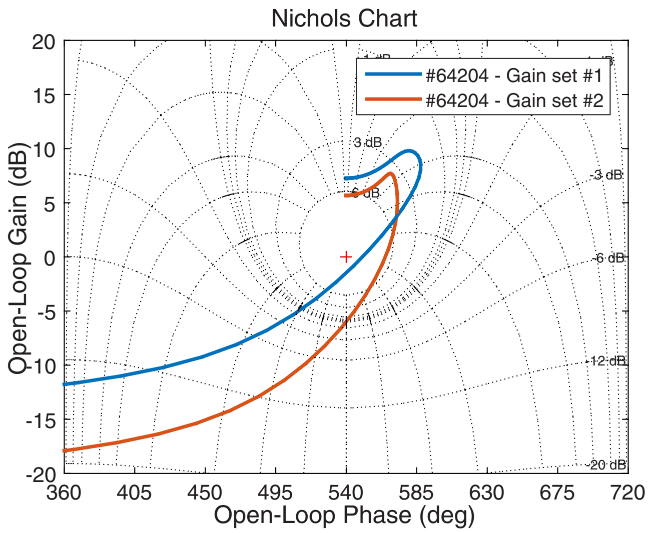

Figure 8. Nichols diagrams for the equilibrium #64204 at $t = 3.5$ s. The blue trace is the diagram obtained when the ITER-like VS parameters are set equal to (3), while the red trace is the diagram for the parameters specified in (4).

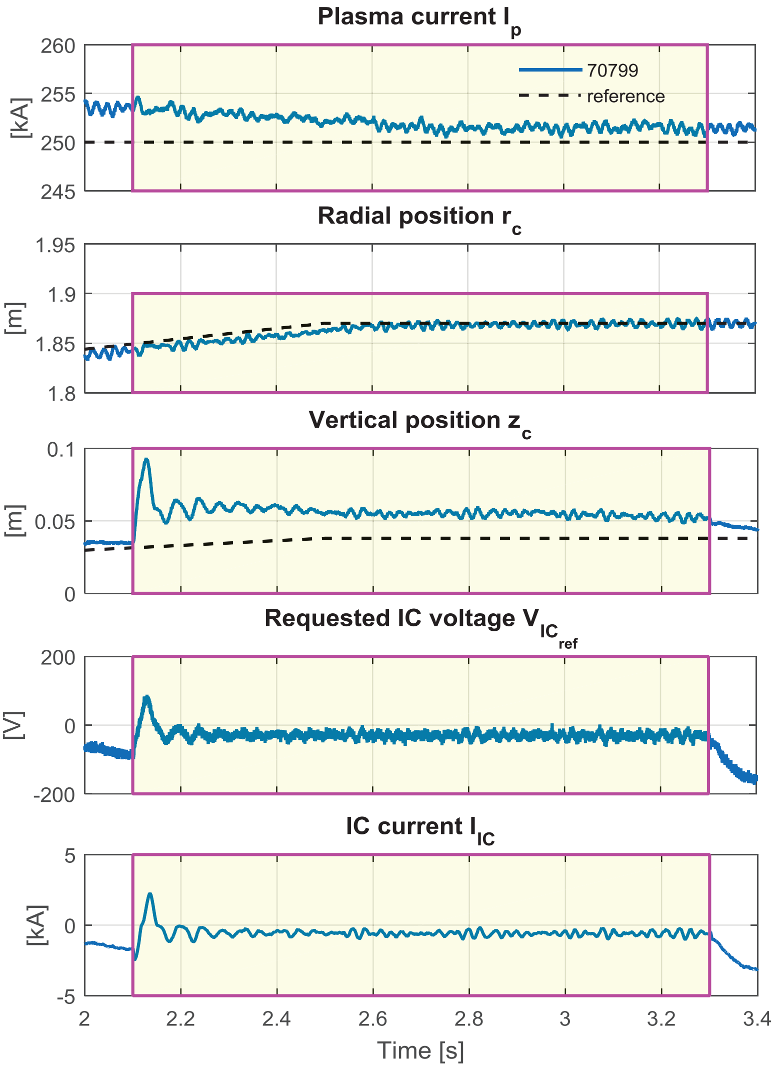

Figure 9. EAST pulse #70799. During this pulse the ITER-like VS was enabled from $t = 2.1$ s for 1.2 s. In this time window only the plasma current I_p and the radial position of the centroid r_c were controlled in closed loop using the *RZIP* algorithm, i.e. z_c was not controlled (indeed, for z_c the dashed black reference is not tracked). This experiment confirmed that the ITER-like VS achieves to stabilize the plasma column by controlling the plasma vertical speed v_c and the I_{IC} current, without the need of the plasma shape and position controller; hence it achieves the desired decoupling between the two control systems.

It results that the proposed MIMO approach relies on a full matrix M, rather than a sparse one. Moreover, the controlled variables are not limited to the position of the X-point and the flux differences along the desired plasma boundary; indeed the descriptors of the flux expansion in the divertor region can be also controlled, in order to indirectly control the heat load (see [1] for more details).

However, in order to effectively apply the *XSC-like* approach to EAST, it is necessary to decouple the vertical stabilization from the plasma current and shape control. Indeed, when designing the integrated plasma shape and flux expansion MIMO controller, in [1] it is assumed that the plasma is vertically stabilized on the fastest time scale as possible, according to the capabilities of the actuator and of the data acquisition system (see also [9, section 3]).

As a matter of fact, the control algorithms implemented in the EAST VS system described in section 2.1 do not guarantee the required decoupling between vertical stabilization and plasma shape control.

As an example, let us consider EAST pulse #56603, which was a single-null plasma at $I_\mathrm{p} \cong 235$ kA. At $t = 2.6$ s the plasma is controlled using the current-driven PID **(vs1)** to vertically stabilize the plasma, and the *RZIP* control algorithm **(spc1)** in order to track the position of the plasma centroid. The estimation for the growth rate γ at $t = 2.6$ s carried out with the CREATE-NL [17] equilibrium code gives $\gamma \cong 1141$ s^{-1}. Exploiting the plasma linear model provided by the create tools described in [1, section 3.1], it is possible to estimate how the unstable eigenvalue is modified—and eventually stabilized—by the EAST magnetic control system. It turns out that, by closing only the current-driven PID, the growth rate is *slowed down* to $\gamma \cong 15$ s^{-1}; hence using the **(vs1)** algorithm, the VS system alone is not capable to vertically stabilize the plasma column. Overall vertical stabilization, is achieved by closing also the *RZIP*. Indeed, closing also this controller, the maximum eigenvalue of the closed loop system obtained using the plasma linear model is equal to $\sim -10^{-4}$, which implies (rather marginal) closed

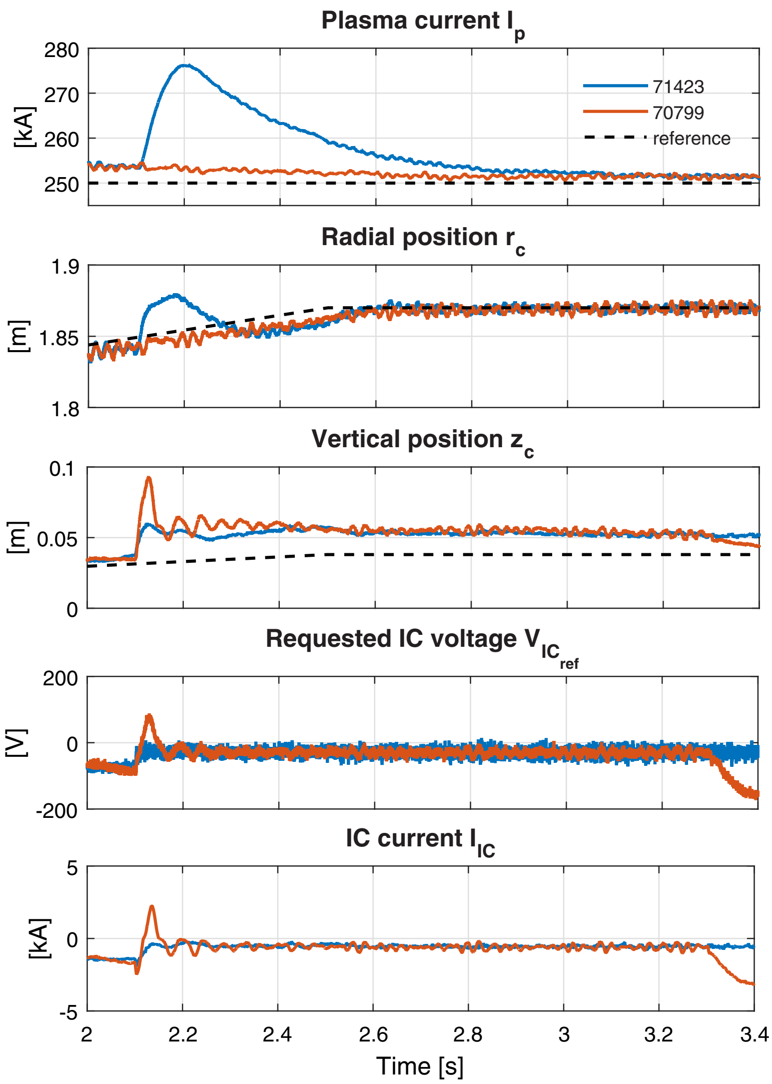

Figure 10. Tuning of the ITER-like VS controller. This figure shows a comparison between the EAST pulses #70799 and #71423. The control parameters in (2) used for the latter pulse were tuned exploiting the CREATE linear model, with the aim of reducing the amplitude of the oscillations on both z_c and I_{IC}.

loop stability. Exploiting the CREATE modeling tools, it is also possible to verify that vertical stabilization is achieved by closing the PID on the *IC* circuit, and by closing only the loop on the vertical position of the plasma centroid provided by the *RZIP* algorithm. If we consider this case, the resulting maximum eigenvalue in closed loop is $\sim -10^{-2}$. Hence, within the existing architecture of the EAST magnetic control, plasma vertical stabilization is achieved by combining both the plasma position and shape controller and the VS system. It turns out that the two system are strongly coupled, and that the design of the plasma shape controller cannot be carried out without explicitly taking into account the VS system. Experimentally *RZIP* control algorithm was used during the ramp-up phase, and the plasma shape control was then switched to isoflux as soon as a single null configuration was reached. However, the VS system and plasma shape control were strongly coupled also when isoflux was used during pulse #56603. Indeed, in simulation it was not possible to simply modify the isoflux gains without affecting the overall stability [1].

As a further example of coupling between VS and plasma shape control, let us consider the EAST pulse #69516 at $t = 2.5$ s. In this pulse the *IC* coil was commanded by the voltage-driven PID **(vs2)** while the enabled plasma shape and position control was *RZIP*, as for the pulse #56603. Also in this case, the VS system alone is not capable to stabilize the plasma, since when we close the voltage-driven PID on the plasma linearized model the growth rate goes from $\gamma \cong 1032$ s^{-1} to $\gamma \cong 501$ s^{-1}. For this specific plasma equilibrium, when closing also the *RZIP* loop, the closed loop system remains unstable. In particular, three unstable eigenvalues appear: one corresponding to the *slowed down* vertical unstable movement, equal to $\sim$504 s^{-1}, and two complex ones, whose estimated natural frequency is $\omega \cong 645$ rad s^{-1}. Such a model-based analysis carried out with the CREATE-NL linear model is in good agreement with the experiment. Indeed, figure 4 shows the time evolution of z_c during the EAST pulse #69516. As confirmed by the model, once the plasma is sufficiently elongated, right after $t = 2.45$ s, the vertical instability starts to grow with an oscillatory mode, whose experimental frequency is $\sim$126 rad s^{-1}. It should be noticed the difference between the estimated value and the experimental one for the natural frequency of the unstable mode is significant; however it should be remarked that, being the closed loop system unstable, using the plasma model around the equilibrium at $t = 2.5$ s gives just a rough estimation about this natural frequency during the dynamic evolution.

Similar conclusions as the one discussed above can be drawn also in the case of the bang–bang VS and/or isoflux plasma shape controller.

The need of decoupling the VS system from the plasma shape controller, in order to independently design of the two control systems, has motivated the deployment of the ITER-like VS algorithm described in section 3. Such an algorithm aims at vertically stabilizing the plasma column, i.e. control to zero v_c, delegating the control of z_c to the plasma shape controller. Moreover, the ITER-like VS tries also to minimize the control effort, by controlling to zero the current in the *IC* circuit.

3. ITER-like vertical stabilization system

In order to achieve the decoupling between the VS and the plasma shape and position control systems, as required by the XSC-like design approach introduced in section 2.2, a ITER-like solution [12, 13] for the VS system has been deployed at EAST.

The proposed solution computes voltage requests for the *IC* power supply according to the simplified block diagram shown in figure 5.

In particular, the voltage request $V_{IC_{\mathrm{ref}}}$ is computed as a linear combination of the plasma vertical speed v_c and of the current flowing in the *IC* circuit. According to the scheme reported in figure 5 and taking into account (2), $V_{IC_{\mathrm{ref}}}$ is computed as

$$V_{IC_{\mathrm{ref}}}(s) = \frac{1+s\tau_1}{1+s\tau_2} \cdot \left(K_v \cdot \bar{I}_{p_{\mathrm{ref}}} \cdot \frac{s}{1+s\tau_z} \cdot Z_c(s) + K_{IC} \cdot I_{IC}(s) \right), \qquad (2)$$

where $I_{IC}(s)$ is the actual value of the current in the in-vessel coil, while $\bar{I}_{p_{\mathrm{ref}}}$ is the nominal value for the plasma current at each time instant. The parameters of the control algorithm are

- K_v, which is the plasma speed gain (scaled by $I_{p_{\mathrm{ref}}}$);
- K_{IC}, which is the *IC* current gain;
- τ_1 and τ_2, which are the time constants of the lead compensator. Such a compensator is needed to adjust the closed loop parameters of the VS system, in order to obtain the desired values for the stability margins and the closed loop bandwidth [18] . Note that, in order to have a lead compensator, it is $\tau_1 > \tau_2$.

The plasma current reference value $I_{p_{\mathrm{ref}}}$ is needed to accordingly scale the speed gain K_v, in order to adapt the overall gain to different values of I_p. This adaption of the speed gain K_v as a function of $I_{p_{\mathrm{ref}}}$ could be avoided if the EAST magnetic diagnostic would estimate $\frac{\mathrm{d}(z_c I_\mathrm{p})}{\mathrm{d}t}$, rather than z_c, as it is done at JET [19]. Indeed, once $\frac{\mathrm{d}(z_c I_\mathrm{p})}{\mathrm{d}t}$ is computed as linear combination of the measurements acquired from the magnetic probes [20], also z_c can be retrieved by means of integration.

In order to show the robustness of the proposed approach with respect to variations of the magnetic equilibrium, we have exploited the CREATE-NL plasma linearized model. In particular, robust stability can be then assessed by using the Nichols chart [18] of the single-input-single-output (SISO) transfer function obtained by opening the control loop at the VS system output. As an example, figure 6 shows the Nichols charts for four different equilibria, whose main parameters are summarized in table 1, and plasma shapes are reported in figure 7. The chart shown in figure 6 have been computed by setting the control parameters as

$$K_v = -2.15 \cdot 10^{-4}, K_{IC} = -5.3 \cdot 10^{-2}, \tau_1 = 1.7\ \mathrm{ms}, \tau_2 = 0.01\ \mathrm{ms}, \qquad (3)$$

and by considering the following pure delay model for the power supply of the *IC* circuit

$$V_{IC}(s) = V_{IC_{\mathrm{ref}}}(s)\mathrm{e}^{-\delta_{\mathrm{PS}} s},$$

where $V_{IC_{\mathrm{ref}}}(s)$ is the voltage request computed by the VS controller, while $V_{IC}(s)$ is the actual voltage applied by the power supply to the *IC* circuit. The power supply delay is $\delta_{\mathrm{PS}} = 550\ \mu$s, and it has been experimentally estimated during dry-run pulses.

From the considered example, it follows that the proposed ITER-like VS is capable to achieves plasma stabilization for all the four different equilibria. For three cases out of four, the phase margin is greater the 40 degrees, and also the gain margins guarantee robustness against either a doubling or a halving of the open loop gain. It should be noticed that, for the equilibrium #64204 at $t = 3.5$ s, which has the higher growth rate among the one considered in table 1, although the closed loop system is still stable, the margins significantly worsen. In this case, the performance can be improved by optimizing the controller parameters for this specific equilibrium. As an example, figure 8 compares the Nichols diagram obtained with (3) with the one obtained tuning the gains as

$$K_v = -2.0 \cdot 10^{-4}, K_{IC} = -4.5 \cdot 10^{-2}, \tau_1 = 1.0\ \mathrm{ms}, \tau_2 = 0.01\ \mathrm{ms}. \qquad (4)$$

As a more general solution, an adaptive algorithm capable of adjusting the VS gains according to the experiment should be envisaged as one of the possible future improvements of the ITER-like VS system at EAST, as it will be discussed in the conclusive section.

4. Experimental results

In this section we present the results obtained during the commissioning and tests of the ITER-like VS system at EAST during the 2016 experimental campaign.

The first presented experiment is aimed to prove that the control algorithm (2) is capable to vertically stabilize the plasma column without the need of the plasma shape and position controller, as predicted by the model-based analysis presented in section 3. In order to do that, during pulse #70799, the ITER-like VS was enabled from 2.1 s to 3.3 s. During the same time window, only I_p and r_c were controlled in closed

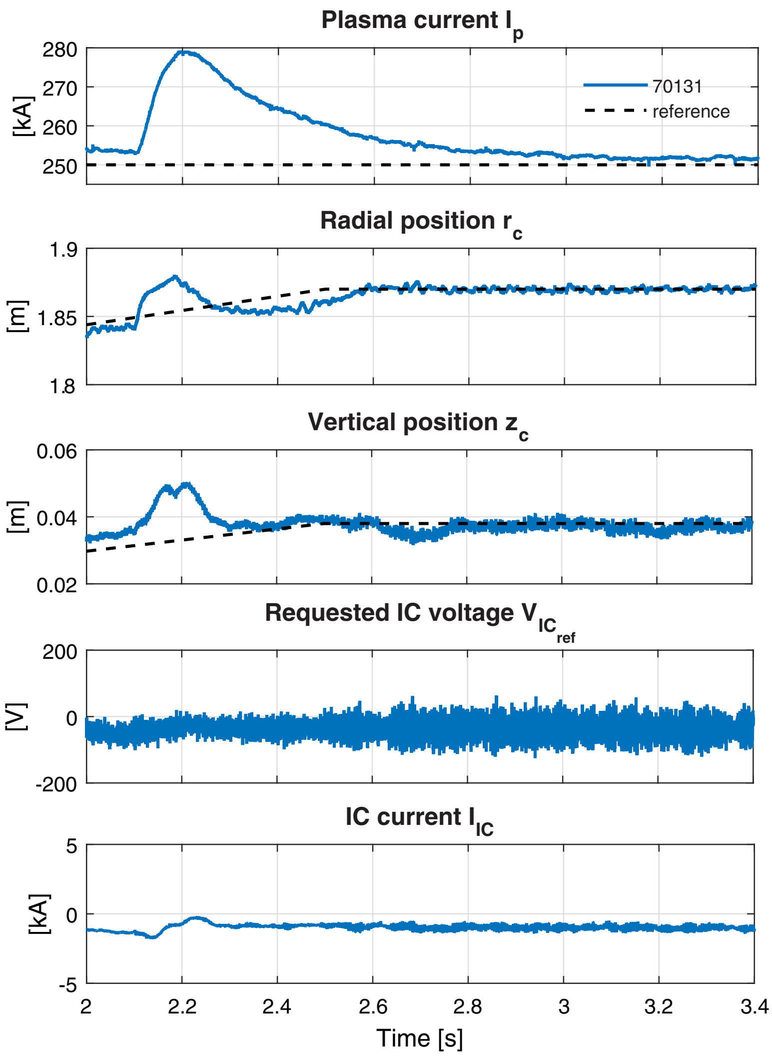

Figure 11. EAST pulse #70131. During this pulse the *RZIP* controller was used also to control z_c.

loop, using the *RZIP* algorithm; that is the loop on z_c was left open.

The experimental result for this pulse are shown in figure 9, where the time traces for I_p, r_c, z_c, $V_{IC_{\mathrm{ref}}}$, and I_{IC} are reported. It should be noticed that, after the initial transient, z_c does not exhibit any exponential drift, meaning that stabilization is achieved without directly controlling the position. Moreover, the current in the control circuit is kept small.

The control parameters of the ITER-like VS used during the pulse #70799 were finely tuned exploiting the CREATE linear model, with the aim of reducing the amplitude of the oscillations on both z_c and I_{IC}. The new set of parameters was set equal to (3), and was used during the EAST pulse #71423. A comparison between the pulses #70799 and #71423 is shown in figure 10, where the ITER-like VS was enabled from 2.1 s to 3.3 s in both cases.

Note that, during pulse #71423, the overall closed loop behavior exhibit less oscillations, regardless the fictitious disturbance that was induced on the plasma current by a bump on the correspondent control loop.

Finally, figure 11 reports the experimental results obtained during the EAST pulse #70131, where the ITER-like VS was enabled from $t = 2.1$ s until the end of the pulse, and the controller parameters were set equal to (3). The loop on z_c of the *RZIP* controller was redesigned, since with the ITER-like VS, this loop does not need to contribute to the vertical stabilization, and used to control also the vertical position of the plasma centroid. Indeed, in figure 11 it can be seen that, regardless the induced disturbance, z_c follows the reference.

5. Conclusions

A solution to decouple the plasma vertical stabilization system from the plasma shape and position controller has been deployed and successfully tested at EAST. The adopted solution is based on the proposal for the ITER VS system originally presented in [12, 13], and it is a key step toward the deployment of a XSC-like MIMO plasma shape controller at EAST. Further development will include the possibility to adapt in real-time the controller parameters for the proposed VS system, in order to avoid the use of different controller settings for different magnetic configurations, as well as the deployment of an an algorithm for integrated control of plasma shape and flux expansion [1].

Acknowledgments

This work has been carried out within the framework of the EUROfusion Consortium and has received funding from the Euratom research and training programme 2014-2018 under grant agreement No. 633053. The views and opinions expressed herein do not necessarily reflect those of the European Commission.

The CREATE team would like to thank Dr Giuseppe Calabró, Dr Flavio Crisanti for the opportunity to work with the ASIPP colleagues at the EAST tokamak, and Prof Giuseppe Ambrosino for his fruitful suggestions.

ORCID

G. De Tommasi https://orcid.org/0000-0002-8509-7176

References

[1] Albanese R. *et al* 2016 A MIMO architecture for integrated control of plasma shape and flux expansion for the EAST tokamak *Proc. 2016 IEEE Multi-Conf. System Control (Buenos Aires, Argentina)* pp 611–6
[2] Kolemen E. *et al* 2015 *J. Nucl. Mater.* **463** 1186
[3] Ariola M. and Pironti A. 2016 *Magnetic Control of Tokamak Plasmas* 2nd edn (Berlin: Springer) (https://doi.org/10.1007/978-3-319-29890-0)
[4] Ryutov D. 2007 *Phys. Plasmas* **14** 064502
[5] Calabrò G. *et al* 2015 *Nucl. Fusion* **55** 083005
[6] Ariola M. and Pironti A. 2005 *IEEE Control Syst. Mag.* **25** 65
[7] De Tommasi G. *et al* 2014 *J. Fusion Energy* **33** 233
[8] Guo Y. *et al* 2015 *Fusion Eng. Des.* **101** 101
[9] De Tommasi G. *et al* 2011 *Fusion Sci. Technol.* **59** 486
[10] Yuan Q. *et al* 2013 *Nucl. Fusion* **53** 043009
[11] Xiao B. *et al* 2016 *Fusion Eng. Des.* **112** 660
[12] Ambrosino G. *et al* 2009 *IEEE Trans. Plasma Sci.* **37** 1324
[13] Ambrosino G., Ariola M., De Tommasi G. and Pironti A. 2011 *IEEE Control Syst. Technol.* **19** 376
[14] Humphreys D. *et al* 2008 *Fusion Eng. Des.* **83** 193
[15] Ambrosino G., Ariola M. and Pironti A. 2007 *IET Control Theory Appl.* **1** 604
[16] Ambrosino G., Ariola M., Pironti A. and Sartori F. 2008 *IEEE Control Syst. Technol.* **16** 1101
[17] Albanese R., Ambrosino R. and Mattei M. 2015 *Fusion Eng. Des.* **96–7** 664
[18] Franklin G., Powell J. and Emami-Naeini A. 2015 *Feedback Control of Dynamic Systems* 7th edn (Upper Saddle River, NJ: Pearson)
[19] Sartori F., De Tommasi G. and Piccolo F. 2006 *IEEE Control Syst. Mag.* **26** 64
[20] Bellizio T. *et al* 2011 *IEEE Trans. Nucl. Sci.* **58** 1497